Accepted Manuscript

Molybdenum isotope fractionation in soils: Influence of redox conditions, organic matter, and atmospheric inputs

C. Siebert, J.C. Pett-Ridge, S. Opfergelt, R.A. Guicharnaud, A.N. Halliday, K.W. Burton

Please cite this article as: Siebert, C., Pett-Ridge, J.C., Opfergelt, S., Guicharnaud, R.A., Halliday, A.N., Burton, K.W., Molybdenum isotope fractionation in soils: Influence of redox conditions, organic matter, and atmospheric inputs, *Geochimica et Cosmochimica Acta* (2015), doi: http://dx.doi.org/10.1016/j.gca.2015.04.007

Molybdenum isotope fractionation in soils: influence of redox conditions, organic matter, and atmospheric inputs

Siebert, C.[1, 3], Pett-Ridge, J.C.[1,2*], Opfergelt, S.[1,5], , R.A. Guicharnaud[6], Halliday, A.N.[1], Burton, K.W.[1,4]

[1]Department of Earth Sciences, University of Oxford, Oxford, United Kingdom

[2]Department of Crop and Soil Science, Oregon State University, Corvallis, OR, United States

[3]Geomar, Helmholtz Center for Ocean Research, Kiel, Germany

[4]Department of Earth Sciences, Durham University, Durham, United Kingdom

[5]Earth and Life Institute, Université catholique de Louvain, Louvain-la-Neuve, Belgium

[6]Agricultural University of Iceland, Keldnaholt, 112 Reykjavik, Iceland

*corresponding author, Julie.pett-ridge@oregonstate.edu, 541-737-1236, 3017 ALS Building, Department of Crop and Soil Science, Oregon State University, Corvallis OR 97331, USA

Abstract

Molybdenum isotope fractionation accompanying soil development is studied across three pedogenic gradients encompassing a range of controlling factors. These factors include variable redox conditions, organic matter content, Fe and Mn oxy(hydr)oxide content, mineral composition, degree of weathering, pH, type and amount of atmospheric inputs, age, climate, and underlying rock type. Soil profiles from the island of Maui (Hawaii) along a precipitation gradient ranging from 850 to 5050 mm mean annual precipitation show a decrease in average soil δ^{98}Mo from -0.04±0.11‰ at the driest, most oxic site, which is indistinguishable from the basalt parent material (-0.09±0.08‰), to -0.33±0.10‰ at the wettest, most reducing site. A suite of 6 Icelandic soils display a broad trend with heavier δ^{98}Mo values (up to +1.50±0.09‰) in soil horizons that are more weathered and have higher organic matter content. Selective extractions of Mo from different soil components indicate that the association with organic matter and silicate or Ti-oxide residue dominates retention of Mo in these soils, with adsorption on Fe and Mn oxy(hydr)oxides playing a lesser role. Across all basaltic soils, δ^{98}Mo values are lighter in soils that exhibit the most net Mo loss relative to the parent material, and δ^{98}Mo values are heavier in soils that exhibit net Mo gains. A well-drained regolith profile in the Luquillo Mountains of Puerto Rico developed on quartz diorite shows heavier δ^{98}Mo values than the parent material (up to +0.71±0.10‰ with an integrated profile average of +0.28±0.10‰) in soil and shallower saprolite, despite overall moderate loss of 28% of Mo relative to the bedrock. However, the deeper saprolite is unfractionated from bedrock (-0.01±0.10‰, quartz diorite bedrock) indicating that rock weathering dissolution processes and secondary clay formation do

not fractionate Mo isotopes. Our data suggest that the Mo mass balance and isotope composition of soils are controlled by redox conditions, organic matter, and atmospheric inputs. In this way Mo isotopes have the potential to react to and record climate driven changes in the weathering environment. The presence of both isotopically light and heavy Mo (relative to parent material) across all sites and within individual soil profiles suggests that it is normal for multiple fractionation mechanisms to operate under the open-system conditions of soils.

1. Introduction

Molybdenum (Mo) is an essential biological micronutrient and a redox sensitive trace metal. As such, the role of Mo as a nutrient has important implications for terrestrial ecology because of its function in regulating nitrogen fixation. In sediments, Mo concentrations and isotopic compositions are used to quantify redox conditions in marine environments, both modern and throughout Earth history (e.g. Arnold et al., 2004; Siebert et al., 2005; Poulson et al., 2006; Siebert et al., 2006; Neubert et al., 2008; Pearce et al., 2008; Wille et al., 2008; Gordon et al., 2009). However, a prerequisite for a reliable interpretation of the Mo records in ancient marine sediments as proxies of the paleo-oxygenation status of the oceans is knowledge of the flux and isotopic composition of riverine water delivered from continents to oceans and the processes that control these fluxes (Barling et al., 2001; Siebert et al., 2003). In some cases, the dissolved Mo isotope composition in rivers appears to directly reflect the Mo isotope composition of the catchment lithology (Neubert et al., 2011), but elsewhere, there is evidence for isotopic fractionation (Archer and Vance, 2008; Pearce et al., 2010; Scheiderich et al., 2010).

Riverine isotope signatures only hint at potential terrestrial processes that may control

Mo elemental and isotopic behavior in weathering environments. An analysis of dissolved Mo in rivers representing 22% of global water discharge to the oceans found a discharge-weighted mean δ^{98}Mo of 0.7‰, and a range from 0.15‰ to 2.40‰ (Archer and Vance, 2008). This is heavy compared to silicate rocks, which have a typical range of approximately 0.0 to +0.4‰ (Siebert et al., 2003; Greber et al., 2014; Voegelin et al., 2014). Individual river samples displayed a general trend of higher δ^{98}Mo associated with lower Mo concentrations. A separate study of dissolved Mo in small catchment streams in Switzerland and India paired with bedrock analysis found that δ^{98}Mo values of sedimentary rocks can be much heavier than the previously determined range of silicate continental rocks (Neubert et al., 2011). In these catchments heavy dissolved δ^{98}Mo in rivers may simply directly reflect heavier sources (presumably preferential dissolution of trace sulfides) as opposed to fractionation during weathering or other soil processes. Nearly all river Mo isotope data published to date are restricted to dissolved Mo. Little is known about the Mo isotope signatures of the suspended load and their contribution to the overall Mo isotope signal of rivers.

Molybdenum isotope fractionation associated with chemical weathering has been studied using laboratory bulk rock leaching experiments for both igneous rocks and shale. These experiments suggest that the dissolved Mo preferentially released during incongruent weathering is isotopically heavy, consistent with heavy riverine Mo isotope data (Liermann et al., 2011; Voegelin et al., 2012). However, aside from a single soil data point (Voegelin et al., 2012), the various processes that may govern soil Mo isotope signatures have not been studied.

Understanding the behavior of Mo isotopes in soil first requires an understanding of Mo behavior and speciation in this environment. During primary mineral formation in basaltic and granitic igneous rocks, Mo is incorporated into dominant primary mineral phases, volcanic glass,

and also in minerals containing Ti and Fe, such as ilmenite, titano-magnetite, and sphene (Manheim and Landergren, 1978; Arnorsson and Oskarsson, 2007). Concentrations of Mo in soil vary substantially (0.01 to 17 $\mu g\ g^{-1}$) with an average of 1.8 $\mu g\ g^{-1}$, but patterns in Mo abundance or leaching from soils have not been broadly studied (Kabata-Pendais, 2011). The dominant dissolved species of Mo in oxygenated soil solutions is the highly soluble molybdate anion (MoO_4^{2-}, Mo in +6 oxidation state), with molybdic acid ($H_2MoO_4^0$) and its oxyanion ($HMoO_4^-$) increasingly present at lower pH (Alloway, 2013).

Molybdenum soil geochemistry is thought to be dominated by adsorption processes at the solid-water interface and by ionic competition for binding sites (e.g. Wu et al., 2000). Laboratory studies show that Mo adsorption to crystalline and poorly crystalline Al and Fe oxides, as well as clays, is greater at low pH extending to a pH range of 4 to 5, with a rapid decrease in adsorption above a pH of 5 and very little at pH 7 (Goldberg et al., 1996). This agrees with agricultural field studies showing that calcium carbonate application (liming) increases soil Mo bioavailability (Gupta, 1997). Some organic substances have an affinity for Mo (Wichard et al., 2009; Kabata-Pendais, 2011) and, consistent with this finding, some humus-rich soils appear to accumulate Mo (McBride, 1994). Precipitation of Mo from the aqueous phase in soils is assumed to play a minor role in most soils (Gupta, 1997). However, in aquatic environments under sulfidic conditions, Mo is removed from the aqueous phase when MoO_4^2 forms Mo-S compounds with Mo in +4 or +5 oxidation state (e.g. Dahl et al., 2013).

Specific mechanisms that may cause fractionation of Mo isotopes in weathering and soil environments include changes in coordination from tetrahedral to octahedral, kinetic effects during metal-ligand bond dissociation, ion specific diffusion rate differences, and equilibrium effects due to varying bond strengths between metal complexes (Malinovsky et al., 2007a;

5

Goldberg et al., 2009; Kashiwabara et al., 2009). Experimental work on Mo adsorption on Mn and Fe oxyhydroxides, as well as observations in nature, point to the preferential adsorption of light isotopes (Siebert et al., 2003; Barling and Anbar, 2004; Malinovsky et al., 2007b; Wasylenki et al., 2008; Liermann et al., 2011; Goldberg et al., 2012). The molybdate oxyanion adsorbs to the solid phase through an inner sphere bond (ligand-exchange) (Goldberg et al., 1996; Fontes and Coelho, 2005), possibly accompanied by a coordination change from tetrahedral to octahedral (Bibak and Borggard, 1994; Kashiwabara et al., 2009). Adsorption of light Mo would leave soil porewater heavy in δ^{98}Mo, which is in agreement with measured river water being heavy in δ^{98}Mo (Archer and Vance, 2008; Pearce et al., 2010; Scheiderich et al., 2010; Neubert et al., 2011).

The aim of this study is to investigate Mo isotope fractionation associated with the major soil-forming (pedogenic) processes. We measure δ^{98}Mo in soils, selective soil chemical extracts, and parent material. In particular, this study investigates the influence of each of the following six factors on soil Mo isotopes:.(1) primary mineral dissolution and incongruent weathering, (2) secondary clay mineral formation, (3) Fe and Mn oxyhydroxides, (4) soil organic matter and redox, (5) biological cycling, and (6) atmospheric inputs.

We have chosen well-characterized basaltic and granitic sites in Maui, Iceland, and Puerto Rico, all of which have simple underlying mono-lithologic geology and minimal anthropogenic effects. The suite of sites was carefully chosen to represent a wide range in soil age, mineralogy, degree of weathering, hydrology, and climate. The sites also represent environments that contribute disproportionately large chemical weathering fluxes globally. To assess controls on Mo isotope compositions, we simultaneously analyzed Mo mobility from each profile relative to parent material weathering inputs, along with Fe, Ti, and Mn mobility, and

other soil properties such as allophane content, C content, and overall weathering status.

Combining soil δ^{98}Mo along with complimentary soil characterization and Mo mobility analysis

from these sites provides a foundation for understanding the behavior of Mo in the weathering

environment, as well as understanding terrestrial Mo fluxes.

2. Study sites

2.1. Hawaii Site Description

Hawaii is an ideal setting for soil weathering research; it is often described as a "natural

laboratory" due to its relatively uniform bedrock, geographic isolation from external

contaminants, and large range in climate and age (e.g. Chadwick et al., 1999). Same-age lava

flows can be followed downslope through different climate regimes, while constant-elevation

transects can cross multiple age lava flows within the same climate regime. The ability to isolate

and examine the effects of specific soil controlling variables has made Hawaii the focus of many

soil development studies (e.g. Chadwick et al., 2003; Chorover et al., 2004; Ziegler et al., 2005).

This study centers on a soil climate gradient on the ~410 ka old shield-building Kula lava

flows and ash located on the northwest slope of the volcano Haleakala on the island of Maui

(Miller et al., 2001; Schuur et al., 2001; Scribner et al., 2006). Because the low slope and the

stability of the remnant shield surfaces minimizes erosion, these soils are considered to represent

100's of ka timescales of pedogenesis, similar to the age of the underlying basalt. These sites

have also been the focus of a study that found Rayleigh fractionation of Fe isotopes with

increasing removal of Fe via reductive dissolution at lower redox conditions (Thompson et al.,

2007). Along the Maui soil climate gradient, the basaltic parent material composition and age,

topographic slope, and vegetation are roughly constant, while precipitation acts as the dominant variable controlling changes in soil development. Soil elevation is ~1300 m, slopes are < 5%, and soil temperature is ~16°C, while mean annual precipitation (MAP) varies from 850 mm to 5050 mm (Schuur et al., 2001). The gradient consists of 8 sites; three of these (Sites 0, 2 and 6) are the primary focus of our Mo isotope analyses. The soil at site 0 is an Andisol with 850 mm yr^{-1} MAP, and the soils at sites 2 and 6 are Inceptisols with 2450 and 5050 mm yr^{-1} MAP, respectively (Table 1) (Soil Survey Staff, 2014). Based on analysis of paleoclimates at various locations on the Hawaiian Islands and particularly along climate gradients, the precipitation levels and differences among sites throughout the Holocene were probably similar to present day (Hotchkiss et al., 2000; Chadwick et al., 2003). The Maui sites 1-6 have undisturbed native forest dominated by a single tree species, *Metrosideros polymorpha*; at the two driest sites, 0 and 1/2, the forest was recently cleared and currently supports pasture grasses such as *Pennistem clandestinum*. A more detailed description of these sites is provided in Schuur et al. (2001) and Miller et al. (2001).

The Maui soil climate gradient is one of the most well characterized soil redox gradients in the world. Schuur et al. (2001) determined the redox potential (Eh) of the 6 wettest (sites 1 through 6) soil profiles on the Maui climate gradient at 3 depths per site (15 cm, 35 cm, and 50 cm), using 10 replicates per depth per site, using monthly measurements for 1 full year. The transition from predominately aerobic to predominately anaerobic (frequently waterlogged) conditions is accompanied by a shift in soil mineralogy and chemistry. At the drier sites (sites 0 to 3), soils contain abundant secondary Fe(III) minerals. Between sites 3 and 4 a redox threshold is observed and at sites 4 to 6, frequent periods of suboxic conditions lead to dissolution and loss of Fe via reductive dissolution of Fe oxyhydroxides (Chadwick and Chorover, 2001; Miller et

8

al., 2001). In contrast, the soil C content increases due to suppressed decomposition of organic matter in reducing soils, from ~ 85 g kg^{-1} at the dry end to 185 g kg^{-1} at the wet end of the soil gradient (Schuur et al., 2001). Soil pH ranges from 3.6 to 4.2 across the Maui soils but is not correlated with rainfall (Schuur et al., 2001). No major basaltic primary minerals remain, and Ti oxides are a significant component in Maui soils, having been concentrated to as much as 30% TiO$_2$ by weight by residual enrichment (Scribner et al., 2006).

2.2. Iceland Site Description

The Icelandic soil profiles are lowland Icelandic soils located in an oceanic boreal climate in the southwest of Iceland. The mean annual precipitation is 1017 mm yr^{-1} and mean annual temperature is 4.7 °C, with a seasonal variability of 15 °C (station Hvanneyri, 1999-2010; Iceland Meterological Office, IMO). The maritime winter climate of Iceland means that these soils are subjected to extensive freeze-thaw cycles relative to other subarctic regions (Orradottir et al., 2008).

Six soil profiles with minimal anthropogenic influence representing common Icelandic soil types were investigated, covering a range of drainage conditions, eolian ash input rates, and degrees of weathering (Arnalds, 2004). These soils have previously been the subject of studies of both weathering processes, nutrient cycling, secondary mineral development, and of Li, Mg, and Si isotope fractionation during weathering (Pogge von Strandmann et al., 2008; Sigfusson et al., 2008; Guicharnaud, 2009; Pogge von Strandmann et al., 2012; Opfergelt et al., 2014). All profiles are located in flat topography and have 0° slope angles. The soils are categorized as follows: Vitric Andosol, Haplic Andosol, Gleyic Andosol, Histic Andosol (2 profiles) and

Histosol, following World Reference Base soil classification (IUSS Working Group WRB, 2014). The Vitric Andosol (V) is a coarse-grained very well drained soil with high content of relatively unweathered volcanic ash and low content of organic matter. Vegetation is limited on the V soil due to lack of water retention and nitrogen availability. The Haplic Andosol (A) is a freely draining soil with abundant allophane and oxalate-extractable Fe, with visible tephra layers in the soil profile. The Gleyic Andosol (GA) is similar to the Haplic Andosol but is somewhat poorly drained, with visible gleying. The two Histic Andosol profiles (HA I and HA) have high organic matter content as well as abundant allophane and oxalate-extractable Fe. The Histosol (H) has greater than 20% C, poor water drainage, and has experienced less eolian input relative to the other Icelandic profiles. The vegetation ranges from sparse (Vitric Andosol) to lush grass (all others). The texture of most soils is silt and silt loam with sand and gravel present in the Vitric Andosol and Gleyic Andosol.

The HA, H, and A profiles are located within the Borgarfjördur catchment, which drains melt water from the Langjökull glacier. The catchment also includes several non-glacial tributaries and the estuary. The GA profile is located within an Agricultural University of Iceland experimental site just north of Reykjavik. The underlying bedrock is tholeiitic basalt of Tertiary age (Haroarson et al., 2008), but the soils are developed from tephra on top of 10 ka glacial till, and the other Icelandic soils studied here likely have similar ~10 ka timescales of pedogenesis dating to the last glacial (Sigfusson et al., 2008). The soils develop downward into the tephra at a rate of approximately 0.4 mm yr^{-1}, but also build upward based on ongoing volcanic ash inputs, resulting in simultaneous congruent dissolution of basaltic glass at the surface and secondary mineral formation in deeper horizons (Sigfusson et al., 2008). The HA, H, A and GA soils receive low influx of volcanic ash of ~0.1 mm yr^{-1} (Sigfusson et al., 2008), but the V soil,

located south of Langjökull in southwest Iceland receives higher ash inputs of ~2 mm yr^{-1} (Arnalds, 2004). Profile HA I is located at Klafastadir in Hvalfjordur, Western Iceland, south of the Borgarfjördur Catchment area. The profile is just 200 m inland from the fjord. The profile includes an identifiable ash layer, "The Landnam layer", ~1 cm thick, (from the 870s AD) at 50 cm depth. Location maps for Iceland soils studied here are shown in Opfergelt et al. (2014).

2.3. Puerto Rico Site Description

In Puerto Rico, soil and saprolite were sampled from the LG1 Guaba ridgetop site within the Rio Icacos watershed, a site previously established by White et al. (1998). The watershed, covered by lower montane wet forest, has a mean annual temperature of 22°C and a mean annual rainfall of 4235 mm with little seasonal variation. The Rio Icacos watershed has been the subject of numerous soil geomorphology and weathering studies that indicate that the surface soil has experienced ~120 ka of pedogenesis (e.g. Brown et al., 1998; Stonestrom et al., 1998; White et al., 1998; Riebe et al., 2003; Pett-Ridge et al., 2009b). The LG1 site is underlain by the Rio Blanco stock, an early Tertiary quartz diorite pluton. The coarse to medium-grained quartz diorite is dominated by plagioclase and quartz, with lesser amounts of biotite and hornblende, <1% K-feldspar and chlorite, and accessory magnetite, sphene, apatite, and zircon. The regolith consists of a ~1 m thick bioturbated soil underlain by ~7 m of saprolite which retains the original bedrock texture. The soil consists of approximately 50% quartz, 15% altered biotite, 30% kaolinite, ~3% goethite and low organic matter content, while the saprolite is dominated by kaolinite (~60%) and quartz (~25%), and contains a small amount of primary plagioclase below 5 m depth (Pett-Ridge et al., 2009b). Selected soil physiographic properties for all soils are shown in Table 1.

3. Methods

In Hawaii and Iceland, soils were sampled by genetic horizon from soil pits down to ~1 meter depth or bedrock. In Puerto Rico, soil and saprolite were hand-augered in depth intervals to the saprolite- bedrock interface at ~850 cm. Samples of fresh parent material (n=5, n=6, and n=1 respectively for Maui, Iceland, and Puerto Rico) were sampled from nearby outcrops. In Maui, samples of first year foliage from the dominant *Metrosideros polymorpha* trees were sampled. Soil samples were oven-dried overnight at 105ºC, sieved at 2 mm, and ground in a boron-carbide or agate mortar and pestle to homogeneity. Bulk soil samples were ashed at 700° C overnight to remove organic matter and oxidize the sample. Digestion of ashed bulk soils was accomplished using a 1:3 HF-HNO_3 acid mix on a hot plate or in an Anton Paar microwave oven. Elemental concentrations including Nb and Zr were measured by ICP-MS. Molybdenum concentrations were determined together with isotopic compositions using MC-ICP-MS (Siebert et al., 2001). Soil properties including cation exchange capacity were determined on unashed soils (Page et al., 1982). A more detailed description of methods for the determination of basic soil properties for the Icelandic soils can be found in Opfergelt et al. (2014), for the Hawaiian soils in Miller et al. (2001) and Schuur et al. (2001), and for the Puerto Rico regolith in Pett-Ridge et al. (2009b).

Bulk soil Mo isotope composition represents the average of a mixture of potentially different isotopic signatures among multiple pools of Mo in soil such as Mo adsorbed to Fe and Mn oxyhydroxides, organically bound Mo, and Mo incorporated into silicate minerals or other chemically resistant phases such as Ti oxides. To assess potential mechanisms driving Mo isotope fractionation in soils we used selective extractions to chemically approximate the Mo

isotope signature associated with each of these phases individually. Several operationally defined components were separated in sequence using the unashed fine earth (<2 mm) fraction of soil samples from selected profiles: the Histic Andosol I, Histosol, Haplic Andosol, and Vitric Andosol in Iceland (HA I, H, A, and V) covering the most weathered to the most unweathered Iceland soils, as well as the driest (site 0) and the wettest (site 6) Maui soils. First, 0.5M HCl was used to target Mo that is water soluble, acid-soluble, and exchangeable as well as Mo associated with poorly-crystalline Fe-oxyhydroxides (Wiederhold et al., 2007). Second, Mo associated with moderately reducible sesquioxides was extracted with NH_2OH-HCl in 1M HCl (Wiederhold et al., 2007). Compared to the citrate-dithionite method, the NH_2OH-HCl extraction has lower trace metal contamination, is less subject to secondary precipitation reactions that could affect the isotope data, and also is known to be effective in extracting Fe-oxides from Fe-rich Hawaiian soils (Pett-Ridge et al., 2007). The third extraction used 30% H_2O_2 in 0.02 M HNO_3 (to prevent readsorption of metals) to extract Mo associated with the oxidizable fraction (organic matter). Finally, the residue, mainly silicates and Ti-oxide phases, was completely digested in a HF-HNO_3 mixture. Extractions were performed on 0.4 g of sieved (<2 mm) and homogenized sample material. All reactions were performed using 8 mL of solution and suspensions were shaken by hand every hour. The 0.5 M HCl extraction step was performed at room temperature (21°C) for 12 hours. The hydroxylamine and H_2O_2 extraction steps were executed using one addition of reagent at 85°C for 4 hours and 16 hours, respectively. Between each step, samples were centrifuged (3400 rpm for 15 min) and supernatant was decanted and subsequently filtered using 0.2 µm syringe top filters. Total digestion of the residue was achieved using 6 mL of HF and 2 mL of HNO_3 in closed beakers at 140°C overnight.

Selective extractions are operationally defined and interpretation of the results can be problematic. Furthermore, care must be taken when interpreting isotope results because the extraction procedure itself might induce fractionation. The extraction methods employed in this study were chosen based on previous experiments that showed no Fe isotope fractionation during stepwise dissolution of Fe oxyhydroxides using 0.5 M HCl (Skulan et al., 2002; Wiederhold et al., 2006). We also employed commonly used extraction techniques for metal partitioning in soil in the case of H_2O_2 in acidic solution for the oxidizable organic matter fraction, and $HF-HNO_3$ for the residue. Both the oxidizable and residue extractions are designed to completely dissolve the target phases, which should minimize the possibility for extraction-induced fractionation. In addition, the low pH at which all these extractions were performed should prevent most secondary precipitation reactions and associated fractionation artifacts and should also minimize fractionation in solution because it favors dissolved octahedral Mo, the same form that adsorbs on Fe-Ti oxide surfaces (Voegelin et al., 2012), which reduces the possibility of fractionation associated with coordination changes.

For Mo isotope measurements, samples were spiked with a [97]Mo and [100]Mo double isotope spike (Siebert et al., 2001). The Mo double spike was added before digestion of bulk soil samples. Complete homogenization of the sample and spike Mo was assured by an oxidation step after digestion (concentrated HNO_3 and H_2O_2). Samples for sequential extractions were double spiked after extraction and determination of the Mo content of the samples by ICP-MS. Mo separation chemistry follows the procedures described in Neubert et al. (2011) and Wasylenki et al. (2008). Because of the highly complex matrix of soil samples, anion and cation exchange chemistry were repeated multiple times until complete separation of Mo from the sample matrix was achieved. In addition, oxidation steps were performed between ion exchange

chemistry steps. Molybdenum isotope measurements were performed on a Nu Plasma HR$^{\circledR}$ MC-ICP-MS at the University of Oxford following the procedure of Siebert et al. (2001). By using a double spike, instrumental and laboratory mass dependent fractionation (after spiking) are resolved from natural mass dependent fractionation. Data are presented in the delta notation using the ^{98}Mo/^{95}Mo ratio (δ^{98}Mo). Isotope measurements are reported relative to an Alfa Aesar ICP standard solution (Specpure® #38791 (lot no. 011895D); for international comparison, we measure the δ^{98}Mo of our in-house standard solution 0.12‰ lighter than NIST SRM 3134 (Greber et al., 2012; Goldberg et al., 2013; Nagler et al., 2014). The external reproducibility of our in-house standard isotope values is at or below 0.1‰ (2 s.d.) for the ^{98}Mo/^{95}Mo ratio. Repeat measurement of USGS shale standard SDO-1 over the course of two years yielded a long-term reproducibility of 0.96 ± 0.12‰ (2s.d.; n=15 (5 individual digestions)). Repeat measurement of USGS basalt standard BHVO-2 over the course of two years yielded 0.12 ± 0.07‰ (2s.d.; n=37 (26 individual digestions)). All soil sample solutions were analyzed twice and reproduced within 0.08‰ (2s.d.). Repeated digestion and analysis of individual bulk soil samples of profiles H and GA yielded a reproducibility of <0.16‰ (2s.d.). Total procedure blanks were at or below 2 ng Mo. The anion resin used has been identified as main source of the observed Mo blank with little significant contribution from reagents used in digestions, column chemistry, and extractions. Molybdenum concentrations were calculated from spiked isotope measurements. USGS standard BHVO-2 yielded an average concentration of 3.7 μg g^{-1}, in good agreement with the value published by Li et al. ((2014); 3.9 μg g^{-1}).

To quantify the net elemental loss or gain relative to the basalt parent material, we applied an open chemical system transport function "τ" (e.g. Chadwick et al., 1990; Anderson et al., 2002; Rasmussen et al., 2011). Element concentrations are normalized to Nb, which has

15

been shown to be the least mobile index element for Hawaiian basalt-derived soils (Kurtz et al., 2000). The mass fraction of an element j added or lost from soil during weathering and soil formation is given relative to the mass of that element in the parent material and is calculated as:

$$\tau_{j,s} = \left[\left(\frac{C_{j,s}}{C_{i,s}} \right) \middle/ \left(\frac{C_{j,p}}{C_{i,p}} \right) \right] - 1$$

where C is the concentration of the element, s is the soil, p is the parent material and i is the least mobile element in this system. Trace element data are not available for HA I and therefore no τ Mo calculations are available for that profile. The τ Ca values are calculated as a measure of the overall weathering status of the soils, with more weathered soils having values closer to -1. Integrated soil profile τ were calculated by summing the individual horizon values (τ_h), each weighted by the product of horizon thickness (z) and density (ρ).

$$\tau_{int} = \left(\sum (\tau_h \rho_h z_h) \right) / (\rho_t z_t)$$

Similarly, integrated soil profile δ^{98}Mo values were calculated by summing the individual horizon values, each weighted by the product of concentration (C_{Mo}), horizon thickness (z) and density (ρ).

$$\delta^{98}Mo = \left(\sum \left(\delta^{98}Mo * C_{Mo} \rho_h z_h \right) \right) / (\rho_t z_t)$$

To examine controls on Mo mobility (τ Mo) in soils, correlations between τ Mo and other soil properties were investigated using linear regressions with a significance defined at $p<0.05$. Specifically, we looked at relationships between τ Mo from individual soil horizons and mobility of other major soil elements (τ Fe, τ Mn, τ Ti), %C$_{organic}$, , τ Ca (an indication of degree of weathering), pH, oxalate or citrate-dithionite extractable Fe (Fe$_{ox}$ and Fe$_d$), and % allophane,

16

(Tables 2, 3, and 4) (Miller et al., 2001; Scribner et al., 2006; Pett-Ridge, 2007; Sigfusson et al., 2008; Lugolobi et al., 2010; Opfergelt et al., 2014). Soil chemical data were tested for normality using the Shapiro-Wilk test; most of the data were found to be normally distributed and the remaining data were transformed prior to regression analysis.

4. Results

4.1. Concentration of total molybdenum in soil horizons and profiles

Soil Mo concentrations for the Maui soil climate gradient range between 0.33 and 15.91 $\mu g\ g^{-1}$, while 5 parent material basalt samples have an mean Mo concentration of 2.32 $\mu g\ g^{-1}$, and a range of 2.19 and 2.97 $\mu g\ g^{-1}$ (Table 2). Icelandic soils have between 0.56 and 6.05 $\mu g\ g^{-1}$ Mo, compared to an average concentration of 1.40 $\mu g\ g^{-1}$ Mo in the basalt parent material (Table 3). Puerto Rico soils have less variability, with between 0.32 and 0.38 $\mu g\ g^{-1}$ Mo in the soil and saprolite, and 0.42 $\mu g\ g^{-1}$ Mo in the quartz diorite parent material (Table 4).

Results of τ calculations are given in Tables 2, 3, and 4 for individual soil horizons, and mass-weighted integrated profile averages are given in Figure 1 and Table 6. In the Maui climate gradient soils, horizons from the uppermost 30 cm of the soil profiles are known to be influenced by Asian dust additions, based on quartz abundances of approximately 5-20% (Scribner et al., 2006). The Mo content and isotope signature of dust is unknown, and we therefore focus our efforts on understanding the influence of rock weathering processes on the lower horizons where the source of soil Mo is expected to be basalt parent material. Excluding the dust-impacted surface horizons, the average τ Mo values vary from -0.21 at site 0, to +0.02 at

17

site 2, to -0.52 at site 6 (Table 6 and Figure 2 a, b, and c). Surface horizons at sites 1/2, 4, and 5 have enrichment in Mo, while the three wettest sites (4, 5, and 6) have the greatest depletion of ~ -0.5 in subsurface B horizons.   Iceland soils exhibit a larger range in depth-integrated average τ Mo values (Table 6 and Figures 2 d, e, f, g, and h). The Haplic Andosol, the Gleyic Andosol and the Vitric Andosol have moderate losses of -0.46, -0.37 and -0.44, respectively. The Histosol shows no significant loss or gain and the Histic Andosol has a moderate gain of +0.19. The Puerto Rico soil and saprolite depth-integrated profile average τ Mo value is -0.28 (Table 6 and Figure 2i).

No significant correlations between τ Mo and either τ Fe, τ Mn, or τ Ti were evident within any individual Maui soil profiles, with the one exception of a strong positive correlation at site 1/2 between both τ Mo and τ Fe ($r^2 = 0.95$, p=0.0005, Electronic Annex Figure 4), and between τ Mo and τ Ti ($r^2 = 0.97$, p=0.0001). Within Maui soils, τ Mo was not significantly correlated with soil % C or τ Ca. In most Maui soil profiles, τ Mo was also not significantly correlated with Fe_{ox} or Fe_d, with the exception of site 1/2, which showed a strong positive correlation with Fe_d ($r^2 = 0.87$, p=0.004)

Iceland soils show marked differences in soil properties between soil horizons with net loss of Mo and other soil horizons with net gain of Mo. Within individual Iceland soil profiles, two soil profiles showed negative correlations between τ Mo and allophane content, in other words more Mo gain in horizons with a lower allophane content (GA, $r^2 = 0.62$, p=0.03; and HA, $r^2 = 0.55$, p=0.03, Electronic Annex Figure 4). Within the HA profile, τ Mo and % organic C were positively correlated (r2=0.82, p=0.003), and across all Iceland soil samples together, a similar positive relationship is observed between τ Mo and % organic C (Figure 4a). A negative

relationship between τ Mo and τ Ca is observed, with more Mo gain in soils with lower τ Ca values (i.e. more weathered soils) (Figure 4b). No correlation between τ Mo and either τ Fe, τ Mn or τ Ti was observed in the Icelandic soils. In the Puerto Rico soil and saprolite profile, no significant correlations were observed between τ Mo and other soil properties.

4.2. Molybdenum isotopes in soil horizons and profiles

Bulk soil Mo isotope values for the three Maui profiles are similar to the parent material composition at site 0, but show differences in certain horizons at site 2 and site 6 from the parent material composition, with a range of δ^{98}Mo values between -0.41‰ and +0.25‰ (Table 5 and Figure 2 a, b, and c). The average Maui basalt parent material δ^{98}Mo composition is -0.09‰ (±0.11‰ 2s.d., n=5). Bulk soil Mo isotope values for six Iceland soil profiles vary over a larger range, from -0.19‰ to +1.50‰ δ^{98}Mo, relative to the basalt parent material -0.03‰ δ^{98}Mo (±0.05‰ 2s.d. n=6) (Table 5 and Figure 2 d, e, f, g, and h). In Puerto Rico, the soil and saprolite vary between -0.03‰ and +0.71‰ δ^{98}Mo, while the quartz diorite bedrock has a value of -0.01‰ δ^{98}Mo (Table 5 and Figure 2 i).

Depth profiles of measured bulk soil δ^{98}Mo values have complex patterns (Figure 2). Maui soils tend to be slightly heavier in near surface horizons and either lighter or near parent material values for δ^{98}Mo at depth. The Histosols or Histic Andosols from Iceland are heavy relative to parent material in near surface horizons, and even heavier in deeper horizons, while less organic matter rich soils have δ^{98}Mo values closer to parent material and less variance with

depth. The Puerto Rico regolith profile was enriched in δ^{98}Mo down to ~4 m depth, and identical to parent material at greater depths.

4.3. Selective extraction of molybdenum from soils

Selective chemical extractions were performed on the driest and wettest Maui soil profiles (Site 0 and Site 6), as well as 4 Iceland soil profiles. Mass balance was used to evaluate the extraction procedure. On a Mo concentration basis, in 12 of 28 samples, the concentration of Mo in the sum of the extractions agreed, within uncertainty (with overlapping error bars), with the concentration of Mo in the separately analyzed bulk soil (Electronic Annex Figure 1). Isotopic mass balance for the sum of extractions was also calculated, weighting each δ^{98}Mo value by the proportion of Mo in that fraction relative to the sum. The isotopic mass balance for the sum of extractions agreed within uncertainty with the δ^{98}Mo measured on the bulk soil for 23 out of 27 samples (Electronic Annex Figure 2). In every sample where the concentration mass balance was within uncertainty on the bulk soil (n=12), the isotope mass balance was also within uncertainty of the bulk soil. For 11 additional samples where the concentration mass balance indicated some loss of Mo during the extraction procedure, the isotopic mass balance was within uncertainty of the bulk soil, which suggests that fractionation artifacts associated with Mo loss during the procedure did not affect the measured isotope values. Depth patterns in δ^{98}Mo values of individual extractions (Electronic Annex Figure 3) are largely consistent when comparing horizons for which both the concentration and isotopic mass balance were good, and those where the mass balance for the sum of extractions was not within uncertainty of the bulk values. Only

samples where concentration and isotopic mass balance were in good agreement were used for interpreting the isotopic signature of particular soil phases.

Mass-weighted integrated soil profile Mo pools obtained from the extraction steps that targeted reducible Fe and Mn oxyhydroxide pools were surprisingly low at the driest Maui site, representing 8% for 0.5 M HCl and 15% for $NH_2OH \bullet HCl$ (Table 5). As expected from the near complete loss of Fe and Mn from the system at the anoxic site 6, these pools were even smaller at this site (4% of total Mo). H_2O_2, targeting the oxidizable pool, presumably organic matter, extracted 28-49% of the soil Mo at site 0 and 8-32% at site 6. The results show that most Mo in Maui soils is either incorporated within "residue" of these extractions, which includes both soil secondary silicate minerals and Ti-oxides, or associated with the targeted organic matter phase, and that the relative fraction of Mo associated with the residue is much higher in the reducing profile.

The Icelandic soils were similar to Maui soils in that the Mo pool in the 0.5 M HCl and $NH_2OH \bullet HCl$ extractions is one of the smallest pools, and most of the Mo was in the residue or oxidizable fractions. Overall the H_2O_2 extraction in the Icelandic soils represented nearly half of the total soil Mo except for the Vitric Andosol where it was 15-20%. In the Icelandic Histic Andosol I (HA I) soil profile, 0.5 M HCl and $NH_2OH \bullet HCl$ extracted 12-35% and 7-14%, respectively, of the total Mo pool, while H_2O_2 extracted between 39% and 59% of the total Mo (Table 5). There is a general trend in the Icelandic soils, wherein the well drained, low organic matter, high τ Ca Vitric Andosol has Mo predominantly associated with the residue, and the poorly drained, high organic matter, low τ Ca Histosol has Mo predominantly in the oxidizable fraction (Table 5). The Haplic Andosol, which is intermediate between those two end-members in soil properties, has roughly equal proportions of Mo in oxidizable and residue fractions.

21

Soil δ^{98}Mo values of the individual extraction pools show fractionation in Mo isotope values from that of the bulk soil (Table 5 and Electronic Annex Figure 3). However, depth trends in δ^{98}Mo for extractions tend to follow the bulk soil isotope compositions. In the oxic site 0 Maui profile, 0.5 M HCl extracted Mo has heavier δ^{98}Mo than the parent rock (albeit close to the analytical error), whereas in the anoxic site 6 profile, the 0.5 M HCl extraction is indistinguishable from the parent rock. The $NH_2OH \cdot HCl$ extraction did not have enough Mo to be analyzed successfully for its isotope composition in either soil. The δ^{98}Mo of the H_2O_2 extracted pool in the Maui soils is more complex. In the site 0 oxic soil profile, surface soil H_2O_2 extracted Mo has δ^{98}Mo similar to parent rock, but two subsurface horizons have δ^{98}Mo values that are heavier than the parent rock. In contrast, in the site 6 anoxic Maui soil profile, δ^{98}Mo of the H_2O_2 extracted pool is heavier than that of the parent rock at the surface, and lighter than that of the parent rock at depth.

In the Icelandic soils, the δ^{98}Mo of the H_2O_2 extracted pool is usually heavier or similar to that of the bulk soil (Table 5 and Electronic Annex Figure 3). The H_2O_2 extracted "organic pool" also usually has a heavier, more fractionated isotope composition compared to the parent material value, whereas the extraction residue tends to have a less fractionated isotopic composition closer to the parent material δ^{98}Mo value. We were not able to analyze the either the 0.5 M HCl and the hydroxylamine extraction steps for their Mo isotope compositions.

5. Discussion

5.1. Overview of observed soil δ^{98}Mo and Mo mobility

Across a soil redox gradient in Maui the net result of open-system soil Mo cycling is the retention of light Mo isotopes under reducing soil conditions while less fractionated Mo, relative to the parent material, is retained under oxic soil conditions (Table 5 and Figure 2 a,b,and c). Thus varying redox-conditions in soils can result in distinct Mo isotope signals. In addition, distinct Mo isotope signals appear to be related to overall Mo mobility in soils such that greater loss is associated with greater fractionation. Figure 3a illustrates this trend across all Maui bulk soil samples, where δ^{98}Mo values in soils that have lost the most Mo relative to parent material have the lightest δ^{98}Mo values, while soils that have lost less Mo, or even gained Mo, have heavier δ^{98}Mo values than their parent material. Icelandic soils follow this same general pattern (Figures 2 d, e, f, g, and h and 3b). In addition to the general tendency for soil δ^{98}Mo values to be related to total Mo mobility, our data show that the soil δ^{98}Mo values are related to the weathering status and organic matter content of the soils. Total reserve in bases (TRB) is the sum of soil Ca, Mg, Na, and K content ($cmol_c kg^{-1}$), and it reflects a combination of two key pedogenic factors, with both increased weathering and increased organic matter content driving lower TRB values, through either leaching loss or dilution (Herbillon, 1986). Considering all measured individual soil horizons from Maui, Iceland and Puerto Rico together, soils with high TRB show little Mo isotopic fractionation, while soils with lower TRB show increasingly large fractionation, both heavy and light (Figure 3c). Soils with high TRB show moderate losses of Mo, while soils with lower TRB show either gain or loss of Mo depending on organic matter content and redox conditions (Figure 3d).

Overall, the results of our soil δ^{98}Mo analyses using samples from monolithologic basalt and quartz diorite catchments clearly confirm that Mo isotope fractionation takes place in soils as a result of pedogenic processes. We find both heavy and light soil δ^{98}Mo values, suggesting that

23

multiple processes act to fractionate Mo in the terrestrial weathering environment. In the following discussion, in section 5.2 we examine controls of Mo mobility in soils, and in section 5.3 we consider the likely importance and influence of each of the following six factors on Mo isotope fractionation: (1) primary mineral dissolution and incongruent weathering, (2) secondary clay mineral formation, (3) Fe and Mn oxyhydroxides, (4) soil organic matter and redox, (5) biological cycling, and (6) atmospheric inputs.

5.2. Controls on Mo mobility in soils

Previous work indicated that reductive dissolution of Fe-oxides is the main mechanism for Fe loss from the wetter Maui soils (Thompson et al., 2007), and the τ values for Fe and Mn of these soils clearly show increasing loss from the soil profile with decreasing redox potential, resulting in near complete loss of Fe and Mn in the most reducing profile (Figure 1). In contrast, τ values for Mo indicate only moderate loss with decreasing Eh (up to 41% or 52%, depending on whether dust-impacted surface horizons are included (Table 6)). During soil leaching MoO_4^{2-} is mobile under oxic conditions, but adsorption of Mo to Fe-and Mn-oxyhydroxides is in general expected to limit overall loss of Mo from soils (Bibak and Borggard, 1994; Goldberg et al., 1996; Lang and Kaupenjohann, 1999; Xu et al., 2013). Therefore, as Fe and Mn oxyhydroxides undergo reductive dissolution and removal, we expected that a concomitant decrease in soil Mo content would be apparent as Mo sorbed to Fe- and Mn-oxyhydroxide would be released and made available for leaching. Surprisingly, this was not the case. There is no simple systematic correlation in our data between the loss of Fe (or Mn) and Mo. The pool of Mo sorbed to Fe and Mn oxides is small relative to total soil Mo for all profiles (Table 5), which partly explains the

lack of correlation between Mo and Fe or Mn. Evidently, Mo is retained in the soil by other means, and/or leached Mo is replaced by higher atmospheric Mo inputs at the reducing site.

Similar to Maui soils, the elemental mobility of Mo in Iceland soils is not strongly related to that of Fe or Mn. In the Iceland soils, the individual horizon Mo τ values show gains in some cases, and somewhat wider variation overall, from -0.6 to +1.6 (Figures 2d, e, f, g, and h) and Table 3). The gains of Mo in the HA and H soils are associated with both higher organic matter content and lower τ Ca (meaning more weathered soil) (Figure 4a and b). Our observation of a negative correlation of τ Mo with allophane content indicates that adsorption on allophane is not driving Mo retention in these soils (Electronic Annex Figure 4). Instead, the results from the histic Iceland soils suggest that high soil organic matter content is implicated in Mo retention. Volcanic ash deposition could also add Mo to surface soils, but the Mo/Nb ratio of recent ash is similar to the basalt parent material(Moune et al., 2012), and thus would not shift Mo τ to positive values.

The overall patterns in Mo τ values as well as the larger fractions of Mo in H_2O_2 extractions for the soils studied here lend additional support to previous research highlighting the importance of organic matter retention of Mo in soil and sediments e.g. (Kabata-Pendais, 2011; Glass et al., 2013). In addition, soil organic matter can not only increase the overall retention of Mo in soil, but simultaneously, soil organic matter coatings on Fe oxides can reduce the sorption capacity of Fe oxides (Lang and Kaupenjohann, 2003). Molybdenum has a strong affinity specifically for catechol groups in soil organic matter tannin and tannin-like substances, and during complexation, Mo is thought to change from tetrahedral to octahedral coordination (Wichard et al., 2009). Retention of Mo in soil by binding to organic matter therefore can not

only serve as a major control on overall Mo mobility, but also is a likely candidate for fractionation of Mo isotopes in the process (Lang and Kaupenjohann, 2000).

5.3. Controls on Mo isotopes in soils

5.3.1. Role of primary mineral dissolution and incongruent weathering

Mo isotope fractionation associated with differential dissolution rates of minerals, yielding heavy dissolved Mo, has been observed for marine sedimentary rocks and in the case of disseminated molybdenite and pyrite in igneous and metamorphic rocks (Malinovsky et al., 2007b; Neubert et al., 2011). Therefore molybdenum isotope fractionation in soils may occur through incongruent mineral dissolution alone if sulfides are present. Although it is unknown if trace molybdenite and pyrite are present in the basalt and quartz diorite parent rocks studied here, our δ^{98}Mo soil data contradict such a mechanism for the investigated profiles because Mo isotopes are unfractionated in the early stages of weathering (Figures 2 g, h, and deep saprolite in Figure 2i). Sulfide minerals with heavy δ^{98}Mo (e.g. Malinovsky et al., 2007b) would dissolve rapidly via oxidative dissolution and be highly mobile upon entering an initial weathering environment, which has a lower sorption capacity compared to more developed soils. This would leave the remaining soil residue with light δ^{98}Mo and create very negative τ Mo values given the high concentrations of Mo in sulfide minerals. In contrast, τ Mo data presented here show a range from intermediate losses to gains, and many of the soil samples have heavier δ^{98}Mo than the parent rock. These results indicate that primary mineral dissolution and differential weathering between minerals are not a dominant control on the soil Mo isotope results reported here.

5.3.2. Role of clay mineral formation

A further process that could fractionate Mo isotopes in soils is the formation of secondary clay minerals, a major factor for other metal stable isotope systems like Li, Mg and Si (e.g. Pogge von Strandmann et al., 2012; Opfergelt et al., 2014). The deep Puerto Rico saprolite and Iceland Vitric and Gleyic Andosols represent the least weathered end-member of this study, and thus have experienced less pedogenesis and are expected to more closely reflect secondary mineral formation. These samples have high secondary mineral contents, but can also be expected to have experienced fewer adsorption-desorption cycles and less atmospheric input relative to other soils studied here. Of the samples from the deepest 3 m of the Puerto Rico Saprolite and the Iceland Vitric and Gleyic Andosols, none show evidence of change in their δ^{98}Mo relative to parent material (Figure 2 g, h, and i) although all of them have undergone significant mineral dissolution based on τ Ca. Even after near complete loss of primary mineral plagioclase, hornblende, and biotite and replacement with secondary mineral kaolinite in the Puerto Rico profile (comprising ~75% of deeper saprolite) (Pett-Ridge et al., 2009b), and ~30% Mo loss, no bulk soil δ^{98}Mo fractionation is observed in the deeper 3 meters (Figure 2 i). Therefore, any potential fractionation of Mo isotopes during secondary mineral formation in this profile is either masked by an equal and opposite Mo fractionation effect caused by another process (which seems improbable) or, more likely, only a tiny amount of Mo is associated with a very large amount of clay formation. Regardless, the results again suggest that there is little isotope fractionation associated with primary mineral dissolution, and further strongly suggests

that any potential δ^{98}Mo fractionation associated with secondary clay mineral formation is negligible.

5.3.3. Role of Fe and Mn oxyhydroxides

Iron and Mn oxyhydroxides contribute substantially to the geochemical cycling of Mo in the oceans and are one of the major Mo isotope fractionating phases in the marine environment. Because of the abundance of these oxides in soils, it is straightforward to assume they play a significant role in Mo isotope fractionation in the terrestrial environment. Based on previously demonstrated preferential adsorption of light Mo isotopes on Mn and Fe oxyhydroxides in laboratory settings (Malinovsky et al., 2007b; Goldberg et al., 2009), it could be hypothesized that the lightest bulk soil δ^{98}Mo might be evident in the most Fe-oxide rich soils. However, data from the Maui redox gradient show the opposite trend, with integrated profile values declining from within error of the parent material value at the driest, most Fe-oxide rich site, to -0.33‰ δ^{98}Mo at the wettest, most Fe-oxide poor site (Table 6). In addition, the small fraction of Mo associated with Fe and Mn oxides in the oxic soil profiles suggest that their influence on the bulk Mo isotope composition of soils may be minor. The isotope values of bulk soils are therefore likely to reflect additional processes beyond light Mo retention on Fe oxyhydroxides.

5.3.4. Role of soil organic matter and redox

Recent studies have shown that soil organic matter can have a major impact on Mo cycling and retention in soils (see summary in Xu et al., 2013 and above). We observe a strong

28

positive correlation between τ Mo and % C in the Iceland soils (Figure 4a). We also observe a weaker positive correlation between τ Mo and % C in the much more highly weathered Maui soils (r^2=0.13, p=0.009). δ^{98}Mo is also positively correlated with % C, becoming heavier with increasing % C. In addition, many soils studied here have heavier δ^{98}Mo in organic matter extractions with respect to the bulk soil (Table 5 and Electronic Annex Figure 3). Preferential adsorption and retention of heavy Mo on soil organic matter can explain these observations. Our results therefore suggest that adsorption to soil organic matter plays a major role in retaining Mo, and specifically heavy Mo, in the investigated soils.

We observe an exception to the heavy Mo isotope signal associated with organic matter in the three deepest horizon organic matter extractions in the anoxic site 6 Maui soil, which have lighter Mo than the bulk soil (Table 5 and Electronic Annex Figure 3). The H_2O_2 extraction results may be confounded by the intimate association between organic matter and Fe in basaltic soils (e.g. Chorover et al., 2004; Mikutta et al., 2009), or may reflect extensive chemical processing in the open-system soil environment over 100s of ka timescales with numerous adsorption and desorption cycles. Interestingly, a reducing soil horizon found within the HA profile in Iceland (low %C, low oxalate-extractable Fe content) also has a very light Mo isotope composition (-0.19‰) compared to the horizons above and below (+0.71‰ and +0.63‰, respectively) and is the only subsurface horizon in the HA profile to have experienced moderate Mo loss. This agrees with the Maui redox gradient data and suggests a systematic difference in the soil retention properties between oxic and anoxic soil environments.

5.3.5. Role of Biology

29

It is unknown if plants fractionate Mo isotopes during biological uptake. To our knowledge, only a single plant δ^{98}Mo value has been published. A root sample which was sieved from a topsoil grab sample (-0.33‰) had an isotope composition of -0.14‰ (Voegelin et al., 2012), although it is unclear if that soil sample represents the source of Mo for that root. Bacterial fractionation of δ^{98}Mo values has been observed, with fractionation of between -0.2‰ and -1.0‰ in cells relative to the surrounding solution (Liermann et al., 2005; Wasylenki et al., 2007; Zerkle et al., 2011), but the importance of this mechanism to bulk soil δ^{98}Mo values is not known.

In strong contrast to other rock derived nutrients such as Ca and P, the concentration of Mo in biomass is small relative to the soil, about 200-fold lower (Bowell and Ansah, 1993; Reed et al., 2013), but over long timescales preferential biological uptake of light Mo isotopes could drive soil to heavy δ^{98}Mo values. However this shift would require a removal mechanism that would prevent the light biological Mo from returning to the soil via litterfall or microbial turnover. If there are Mo isotope fractionation effects during plant cycling, the Maui soils are likely old enough to reflect a biological imprint on soil Mo isotope values given less than 100% efficient recycling of Mo. Leaves from the dominant tree *Metrosideros polymorpha* at the Maui sites have an average Mo concentration of 69 ng g^{-1} (Electronic Annex Table 2). Using the aboveground net primary productivity of the Maui soil ecosystems of 400 to 1000 g m^{-2} ha^{-1} (Schuur et al., 2001) and a biomass Mo concentration of 69 ng g^{-1}, we calculate that turnover time for the soil Mo pool (to 50 cm depth) with respect to plant cycling ranges between 22 ka (drier sites) to 52 ka (wetter sites). If, for example, internal recycling of Mo through biomass was 95% efficient with 5% leaching or off-site litter loss per year, the timescale required for plants to shift bulk soil δ^{98}Mo values at the soil profile scale would increase to ~435 or 1043 ka.

The small magnitude of the biological flux relative to the soil pool, together with the fact that plant and microbial Mo is likely internally recycled with minimal leaching loss (Wichard et al., 2009), suggests that the uptake and return of biological Mo as a micronutrient requires long timescales to strongly leverage the profile bulk soil δ^{98}Mo, although plant fractionated Mo isotope values may be more apparent in surface horizons.

5.3.6. Role of additional sources of Mo: Atmospheric Inputs

As soils develop over time, atmospheric inputs have an increasing influence on soil chemical budgets (Kennedy et al., 1998; Porder et al., 2007). Atmospheric inputs affecting the soils studied here include long-range mineral aerosol dust inputs, and sea salt spray incorporated into rainfall (Chadwick et al., 2009; Pett-Ridge et al., 2009a; Opfergelt et al., 2014). Local volcanic ash may also affect the Maui and Iceland soils, but is not expected to alter δ^{98}Mo values relative to underlying parent material due to its very similar composition.

We first consider the possible impact of dust-derived Mo for the Maui soils. Using a dust Mo concentration of 1.8 µg g^{-1}, based on the average worldwide soil Mo concentration (Kabata-Pendais, 2011), a 20% quartz content of Hawaiian dust (Kurtz et al., 2001), and the measured quartz content of the Maui climate gradient soils (Scribner et al., 2006), we calculate that the total % of soil Mo that is dust derived is 14%, 3%, and 9% at sites 0, 2, and 6, respectively. We do not observe a correlation between δ^{98}Mo and % soil Mo potentially derived from dust in the Maui soils, implying that dust is unlikely to be a primary influence on bulk soil δ^{98}Mo values. In contrast, in the Puerto Rico soil and saprolite profile, dust inputs are relatively high due to its Caribbean location downwind of the African dust trajectory. Given a flux of 210 kg ha^{-1} yr^{-1},

31

dust inputs (Pett-Ridge et al., 2009b) to the ~120 ka weathering profile could significantly affect the Mo budget and, potentially, its isotope signature. Evidence of dust impact on the Mo isotopes is not straightforward, however, as the depth profile of δ^{98}Mo does not correlate with the depth profile of dust content based on Nd isotopes (Pett-Ridge et al., 2009b). Long-range dust inputs are not expected to strongly influence the Iceland soils given their young age (<10 ka).

Sea salt-derived Mo may also be added to soil profiles via rainfall but the magnitude and relative importance of these fluxes is not known. A study of Atlantic aerosols found that sea salts generated from the ocean surface can serve as a major source for Mo (Chester et al., 1984), and we expect this Mo to have the heavy seawater δ^{98}Mo value of 2.3‰, which could potentially act as a strong influence on soil δ^{98}Mo values. Controls on the concentration of Mo in rainwater are not well known, but anthropogenic pollution greatly increases dissolved rainwater Mo downwind from areas of fossil fuel combustion or smelting activity, and most published values on Mo concentration in rain are for locations downwind from anthropogenic activity (e.g. Tsukuda et al., 2005). In the Oregon Coast Range, which receives largely unpolluted air masses, we observe a range of Mo concentrations from 4 to 32 pg ml^{-1} in 17 rainwater samples (Marks, 2014). For the Maui soils, using Oregon Coast Range rainfall Mo concentrations, adjusted using Maui annual rain fluxes, the turnover time for the total profile soil Mo pool relative to the range of rainwater Mo inputs is between 17 ka at the wettest site and 688 ka at the driest site.

In the Icelandic soil HA I, soil porewater Na/Cl ratios are almost identical to that of seawater (Pogge von Strandmann et al., 2012), highlighting the potential importance of sea salt inputs, which occur both laterally through rainfall-fed groundwater and from the top down. Given the average range of measured Cl$^-$ concentrations in rainwater collected near this Icelandic soil (Gislason et al., 1996), and given the seawater Cl:Mo ratio of 1.9 x 10^6 and if the sea salt

32

ratio is preserved in precipitation fluxes, Mo in Icelandic rain is likely 1.9 to 9.1 pg ml^{-1}. This translates to 0.02 to 0.09 g ha^{-1} yr^{-1} Mo flux from sea salt, assuming 1000 mm yr^{-1} precipitation. If we use the upper estimate on a time scale of 10 ka (time since last glaciation) this flux of 900 g Mo/ha from sea salt represents approximately 5-9% of the current Mo pool in the Icelandic HA and H soil profiles. Using the seawater δ^{98}Mo value of +2.3‰ and based on the current Mo content of the soil profile, this input of seawater derived heavy Mo alone could shift the soil δ^{98}Mo value from the bedrock value to +0.18‰ in the HA profile and +0.09‰ in the H profile, which could partially account for heavy soil δ^{98}Mo values. The integrated whole profile δ^{98}Mo we observe in the HA and H profiles is +0.31‰ and +0.38‰ (Table 6). In addition to the vertical influx of sea salt through rain, horizontal flow paths through these low lying soils have been proposed as an additional source of rainfall-derived chemistry including heavy δ^7Li values (Pogge von Strandmann et al., 2012). These calculations suggest that sea salt flux may contribute significantly to the observed heavy soil values.

5.3.7 The relative importance of controls on Mo isotopes in soils

This study presents an initial investigation of a wide number of potential processes controlling Mo isotope signatures in the terrestrial weathering environment. Based on the soils investigated here, primary mineral dissolution, incongruent weathering, clay mineral formation, and adsorption by Fe and Mn oxy(hydr)oxides play a minor role in soil Mo isotope fractionation. It appears that the very low Mo concentrations typically found in plants limit the magnitude of potential effects of biological cycling, but direct investigation of this is needed.

Our results highlight the importance of soil organic matter, redox conditions, and atmospheric inputs (which are often uncharacterized) in controlling soil δ^{98}Mo values. Although our results point to relatively complex behavior of Mo isotopes in soils, the recognition of this complexity, does not change two key observations in terms of Mo isotope fractionation that are supported by both the bulk soil and the selective extraction Mo isotope data. First, across a soil redox gradient in Maui the net result of open-system soil Mo cycling is the retention of light Mo under reducing conditions (Figure 2c and 3a). Secondly, δ^{98}Mo values in soils that have lost the most Mo relative to parent material have the lightest δ^{98}Mo values, while soils that have lost less Mo, or even gained Mo, have heavier δ^{98}Mo values than their parent material (Figure 3a and 3b).

6. Implications for global Mo fluxes

Although not a focus of this paper, the fractionation of Mo isotopes in soils by terrestrial weathering raises the question of how soil processes will affect the flux and isotope composition of riverine Mo delivered to the oceans over time. Our results suggest that terrestrial weathering may cause the dissolved Mo input flux to the oceans to differ from that of the average continental crust (~0.0 to 0.4‰; (Siebert et al., 2003; Greber et al., 2014; Voegelin et al., 2014)), an important consideration for the interpretation of the oceanic Mo paleo-proxy. We employed a simplified box model (Siebert et al., 2003) to assess the order of magnitude by which Mo isotope fractionation resulting from soil processes would have to change to be theoretically detectable in the bulk ocean dissolved Mo isotope signature. For this model we assumed a steady state condition using modern fluxes, including a 1.8×10^{8} mol yr^{-1} riverine Mo flux (Archer and Vance, 2008), which translates to a 800 ka residence time for dissolved Mo in the ocean. We

find that the minimum scenario resulting in measurable changes in δ^{98}Mo of the ocean (i.e. >

0.3‰ δ^{98}Mo) on 10 ka timescales would include the reduction (or increase) of dissolved Mo

input to the oceans by ~30% along with a simultaneous change in the δ^{98}Mo of the riverine input

of at least 0.2‰. We also estimate that the turnover time for soil Mo with respect to the riverine

dissolved Mo flux is on the order of roughly 20 ka, assuming a 1 m soil depth, soil Mo content of

1.8 µg g^{-1}, soil density of 1.3 g cm^3, and soil area of 87% of the total land surface. We would like

to point out that this calculation is only intended to provide a rough timescale (at the order of 10

ka) over which soil processes may be reflected in the δ^{98}Mo of the ocean, and an estimate of

changes in parameters necessary to produce such a signal. This does not imply that such a signal

would be necessarily visible in the marine sedimentary record.

Despite the fact that the timescales on which changes in soil processes will influence the

marine Mo isotope signal are limited to the order of 10 ka due to the relatively short turnover-

time for Mo in soil, there are scenarios in which changes in the riverine Mo flux and isotope

composition caused by soil processes could be useful tracers of terrestrial processes. For

example, glacial-interglacial cycles can alter the relative dominance of chemical and physical

weathering, and would have associated changes in precipitation and biological productivity that

could affect degree of soil weathering and soil organic matter content. On a regional scale, these

changes can significantly change the riverine input into restricted basins such as the Baltic or

Black Sea, where there is a high likelihood that the sedimentary record will reflect these changes.

Previous studies have examined molybdenum and other redox-sensitive elements in these basins

at glacial-interglacial timescales (e.g. Jilbert and Slomp, 2013; Scholz et al., 2013). However,

the soil processes governing Mo isotope fractionation will need to be clarified in order to

establish meaningful models in these cases.

7. Conclusions

Molybdenum isotope data for soils reflecting a wide range in climate, pH, Eh, %C, and degree of weathering on both basalt and quartz diorite parent material clearly demonstrate that pedogenic processes fractionate Mo isotopes. A wide range of both light and heavy δ^{98}Mo from -0.41‰ to +1.5‰ was found in bulk soil samples. The range of soils studied here gives a broad view of some of the key processes involved in controlling Mo mobility and isotope fractionation in soils, and the complexity in δ^{98}Mo patterns indicates that more than one fractionation mechanism is at work.

Our finding of a consistent pattern across both Maui and Icelandic soils, where soils with net loss of Mo have lighter Mo isotope ratios and soils with Mo gains have heavier Mo isotope ratios has important implications for the interpretation of Mo isotope data in terrestrial environments. Additionally, we find that the Mo gains in soil profiles relative to parent material inputs are strongly associated with %C content. These results highlight the importance of Mo retention via Mo-organic matter interactions, as has been recently highlighted in both soil, lacustrine, and marine sediment environments (McManus et al., 2006; Wichard et al., 2009; Dahl et al., 2013). Our results also indicate that atmospheric inputs affect soil Mo, and could potentially alter the isotopic signature of bulk soil, especially in older and wetter soils. Together, the observed correlations of Mo retention and isotope fractionation with organic matter (i.e. biological cycling), and the influence of redox conditions and atmospheric inputs raise the possibility that Mo isotopes in soils could potentially reflect the paleo-productivity and paleo-climate conditions a soil has experienced.

Figure Captions:

Fig. 1: Mass weighted profile integrated τ data for Maui soils across the climate gradient, with median Eh values for comparison. Mass weighted profile integrated τ data were calculated excluding dust impacted surface horizons, marked with* in Table 2. Elemental mass transfer τ values, calculated using Nb as a relatively immobile index element, indicate the amount of loss (or gain) of Mo relative to underlying parent material inputs.

Fig. 2: Depth profiles of τ Mo are shown in solid black diamonds, representing the elemental mass transfer (gain or loss relative to underlying parent material inputs) of Mo in Maui soils (a, b, and c); Iceland soils (d, e, f, g, and h); and Puerto Rico saprolite (i). Values greater than 0 indicate gain of Mo, values less than 0 indicate net loss of Mo from the soil. Depth profiles of bulk soil δ^{98}Mo are shown in open black diamonds with dashed lines. Gray bars indicate the δ^{98}Mo $\pm$ 2 s.d. of the parent material for each site. Note the expanded scale used for Iceland and Puerto Rico.

Fig. 3: Elemental mass transfer of Mo in the soil (τ Mo), versus δ^{98}Mo, with gray boxes representing the parent material value with 2 s.d. uncertainty and assuming $\pm 10\%$ uncertainty on τ Mo for (a) Maui soils, and (b) Iceland soils. In (c), the bulk soil δ^{98}Mo for all soils in Maui, Iceland, and Puerto Rico is shown as a function of total reserve in bases (TRB, cmol$_c$ kg^{-1}), which reflects weathering status, with lower TRB values indicating more weathered soils. Gray box represents the range of δ^{98}Mo $\pm$ 2 s.d. for parent material from all three sites. In (d) τ Mo is plotted against TRB, with a gray box representing uncertainty on τ Mo assuming $\pm 10\%$. Error bars on data points represent 2s.d. uncertainty on δ^{98}Mo values.

Figure 4: For all soils in Maui, Iceland, and Puerto Rico, the relationship between elemental mass transfer of Mo (τMo) is plotted against (a) % organic carbon, and (b) elemental mass transfer of Ca (τCa). The Puerto Rico saprolite has extremely low % organic carbon and near

complete loss of Ca (a), and the highly weathered Maui soils have essentially complete loss of

Ca (b).

References

Alloway, B.J. (2013) Molybdenum, in: Alloway, B.J. (Ed.), Heavy Metals in Soils" Trace Metals and Mettaloids in Soils and their Bioavailibility. Springer, New York, pp. 527-534.

Anderson, S.P., Dietrich, W.E. and Brimhall, G.H. (2002) Weathering profiles, mass-balance analysis, and rates of solute loss: Linkages between weathering and erosion in a small, steep catchment. Geological Society of America Bulletin 114, 1143-1158.

Archer, C. and Vance, D. (2008) The isotopic signature of the global riverine molybdenum flux and anoxia in the ancient oceans. Nature Geoscience 1, 597-600.

Arnalds, O. (2004) Volcanic soils of Iceland. Catena 56, 3-20.

Arnold, G.L., Anbar, A.D., Barling, J. and Lyons, T.W. (2004) Molybdenum isotope evidence for widespread anoxia in mid-proterozoic oceans. Science 304, 87-90.

Arnorsson, S. and Oskarsson, N. (2007) Molybdenum and tungsten in volcanic rocks and in surface and < 100 degrees C ground waters in Iceland. Geochimica Et Cosmochimica Acta 71, 284-304.

Barling, J. and Anbar, A.D. (2004) Molybdenum isotope fractionation during adsorption by manganese oxides. Earth and Planetary Science Letters 217, 315-329.

Barling, J., Arnold, G.L. and Anbar, A.D. (2001) Natural mass-dependent variations in the isotopic composition of molybdenum. Earth and Planetary Science Letters 193, 447-457.

Bibak, A. and Borggard, O.K. (1994) Molybdenum adsorption by aluminum and iron-oxides and humic acid. Soil Science 158, 323-328.

Bowell, R.J. and Ansah, R.K. (1993) Trace-element budget in an African savanna ecosystem. Biogeochemistry 20, 103-126.

Brown, E.T., Stallard, R.F., Larsen, M.C., Bourles, D.L., Raisbeck, G.M. and Yiou, F. (1998) Determination of predevelopment denudation rates of an agricultural watershed (Cayaguas River, Puerto Rico) using in- situ-produced Be-10 in river-borne quartz. Earth and Planetary Science Letters 160, 723-728.

Chadwick, O.A. and Chorover, J. (2001) The chemistry of pedogenic thresholds. Geoderma 100, 321-353.

Chadwick, O.A., Derry, L.A., Bern, C.R. and Vitousek, P.M. (2009) Changing sources of strontium to soils and ecosystems across the Hawaiian Islands. Chemical Geology 267, 64-76.

Chadwick, O.A., Derry, L.A., Vitousek, P.M., Huebert, B.J. and Hedin, L.O. (1999) Changing sources of nutrients during four million years of ecosystem development. Nature 397, 491-497.

Chadwick, O.A., Gavenda, R.T., Kelly, E.F., Ziegler, K., Olson, C.G., Elliott, W.C. and Hendricks, D.M. (2003) The impact of climate on the biogeochemical functioning of volcanic soils. Chemical Geology 202, 195-223.

Chadwick, O.A., H., B.G. and Hendricks, D.M. (1990) From a black box to a gray box - a mass balance interpretation of pedogenesis. Geomorphology 3, 369-390.

Chester, R., Sharples, E.J. and Murphy, K.J.T. (1984) The distribution of particulate Mo in the Atlantic aerosol. . Oceanologica Acta 7, 441-450.

Chorover, J., Amistadi, M.K. and Chadwick, O.A. (2004) Surface charge evolution of mineral-organic complexes during pedogenesis in Hawaiian basalt. Geochimica Et Cosmochimica Acta 68, 4859-4876.

Dahl, T.W., Chappaz, A., Fitts, J.P. and Lyons, T.W. (2013) Molybdenum reduction in a sulfidic lake: Evidence from X-ray absorption fine-structure spectroscopy and implications for the Mo paleoproxy. Geochimica Et Cosmochimica Acta 103, 213-231.

Fontes, R.L.F. and Coelho, H.A. (2005) Molybdenum determination in Mehlich-1 and Mehlich-3 soil test extracts and molybdenum adsorption in Brazilian soils. Communications in Soil Science and Plant Analysis 36, 2367-2381.

Gislason, S.R., Arnorsson, S. and Armannsson, H. (1996) Chemical weathering of basalt in southwest Iceland: Effects of runoff, age of rocks and vegetative/glacial cover. American Journal of Science 296, 837-907.

Glass, J.B., Chappaz, A., Eustis, B., Heyvaert, A.C., Waetjen, D.P., Hartnett, H.E. and Anbar, A.D. (2013) Molybdenum geochemistry in a seasonally dysoxic Mo-limited lacustrine ecosystem. Geochimica Et Cosmochimica Acta 114, 204-219.

Goldberg, S., Forster, H.S. and Godfrey, C.L. (1996) Molybdenum adsorption on oxides, clay minerals, and soils. Soil Science Society of America Journal 60, 425-432.

Goldberg, T., Archer, C., Vance, D. and Poulton, S.W. (2009) Mo isotope fractionation during adsorption to Fe (oxyhydr)oxides. Geochimica Et Cosmochimica Acta 73, 6502-6516.

Goldberg, T., Archer, C., Vance, D., Thamdrup, B., McAnena, A. and Poulton, S.W. (2012) Controls on Mo isotope fractionations in a Mn-rich anoxic marine sediment, Gullmar Fjord, Sweden. Chemical Geology 296, 73-82.

Goldberg, T., Gordon, G., Izon, G., Archer, C., Pearce, C.R., McManus, J., Anbar, A.D. and Rehkamper, M. (2013) Resolution of inter-laboratory discrepancies in Mo isotope data: an intercalibration. Journal of Analytical Atomic Spectrometry 28, 724-735.

Gordon, G.W., Lyons, T.W., Arnold, G.L., Roe, J., Sageman, B.B. and Anbar, A.D. (2009) When do black shales tell molybdenum isotope tales? Geology 37, 535-538.

Greber, N.D., Pettke, T. and Nagler, T.F. (2014) Magmatic-hydrothermal molybdenum isotope fractionation and its relevance to the igneous crustal signature. Lithos 190, 104-110.

Greber, N.D., Siebert, C., Nagler, T.F. and Pettke, T. (2012) d98/95Mo values and Molybdenum Concentration Data for NIST SRM 610, 612 and 3134: Towards a Common Protocol for Reporting Mo Data. Geostandards and Geoanalytical Research 36, 291-300.

Guicharnaud, R.A. (2009) Biogeochemistry of Icelandic Andosols, PhD thesis. University of Aberdeen, p. 280.

Gupta, U.C. (1997) Molybdenum in Agriculture. Cambridge University Press, Cambridge, U.K.

Haroarson, B.S., Fitton, J.G. and Hjartarson, A. (2008) Tertiary volcanism in Iceland. Jokull 58, 161-178.

Herbillon, A. (1986) Chemical estimation of weatherable minerals present in the diagnostic horizons of low activity clay soils, in: Beinroth, F.H., Camargo, M.N., Eswaran, H. (Eds.), Proceedings of the 8th International Soil Classification Workshop: Classification, Characterization and Utilization of Oxisols, PArt 1. EMBRAPA, Rio de Janeiro, pp. 39-48.

Hotchkiss, S., Vitousek, P.M., Chadwick, O.A. and Price, J. (2000) Climate cycles, geomorphological change, and the interpretation of soil and ecosystem development. Ecosystems 3, 522-533.

IUSS Working Group WRB (2014) World Reference Base for Soil Resources 2014. International soil classification system for naming soils and creating legends for soil maps. FAO, Rome.

Jilbert, T. and Slomp, C.P. (2013) Rapid high-amplitude variability in Baltic Sea hypoxia during the Holocene. Geology 41, 1183-1186.

Kabata-Pendais, A. (2011) Trace Elements in Soils and Plants. Taylor and Francis Group, Boca Raton, FL.

Kashiwabara, T., Takahashi, Y. and Tanimizu, M. (2009) A XAFS study on the mechanism of isotopic fractionation of molybdenum during its adsorption on ferromanganese oxides. Geochemical Journal 43, E31-E36.

Kennedy, M.J., Chadwick, O.A., Vitousek, P.M., Derry, L.A. and Hendricks, D.M. (1998) Changing sources of base cations during ecosystem development, Hawaiian Islands. Geology 26, 1015-1018.

Kurtz, A.C., Derry, L.A. and Chadwick, O.A. (2001) Accretion of Asian dust to Hawaiian soils: Isotopic, elemental, and mineral mass balances. Geochimica et Cosmochimica Acta 65, 1971-1983.

Kurtz, A.C., Derry, L.A., Chadwick, O.A. and Alfano, M.J. (2000) Refractory element mobility in volcanic soils. Geology 28, 683-686.

Lang, F. and Kaupenjohann, M. (1999) Molybdenum fractions and mobilization kinetics in acid forest soils. Journal of Plant Nutrition and Soil Science 162, 309-314.

Lang, F. and Kaupenjohann, M. (2000) Molybdenum at German Norway spruce sites: contents and mobility. Canadian Journal of Forest Research-Revue Canadienne De Recherche Forestiere 30, 1034-1040.

Lang, F. and Kaupenjohann, M. (2003) Immobilisation of molybdate by iron oxides: effects of organic coatings. Geoderma 113, 31-46.

Li, J., Liang, X.-R., Zhong, L.-F., Wang, X.-C., Ren, Z.-Y., Sun, S.-L., Zhang, Z.-F. and Xu, J.-F. (2014) Measurement of the Isotopic Composition of Molybdenum in Geological Samples by MC-ICP-MS using a Novel Chromatographic Extraction Technique. Geostandards and Geoanalytical Research 38, 345-354.

Liermann, L.J., Guynn, R.L., Anbar, A. and Brantley, S.L. (2005) Production of a molybdophore during metal-targeted dissolution of silicates by soil bacteria. Chemical Geology 220, 285-302.

Liermann, L.J., Mathur, R., Wasylenki, L.E., Nuester, J., Anbar, A.D. and Brantley, S.L. (2011) Extent and isotopic composition of Fe and Mo release from two Pennsylvania shales in the presence of organic ligands and bacteria. Chemical Geology 281, 167-180.

Lugolobi, F., Kurtz, A.C. and Derry, L.A. (2010) Germanium-silicon fractionation in a tropical, granitic weathering environment. Geochimica Et Cosmochimica Acta 74, 1294-1308.

Malinovsky, D., Baxter, D.C. and Rodushkin, I. (2007a) Ion-specific isotopic fractionation of molybdenum during diffusion in aqueous solutions. Environmental Science & Technology 41, 1596-1600.

Malinovsky, D., Hammarlund, D., Ilyashuk, B., Martinsson, O. and Gelting, J. (2007b) Variations in the isotopic composition of molybdenum in freshwater lake systems. Chemical Geology 236, 181-198.

Manheim, F.T. and Landergren, S. (1978) Molybdenum abundance in common igneous rocks and in the Earth's crust, in: Wedepohl, K.H. (Ed.), Handbook of Geochemistry II. Springer, Berlin, p. 87.

Marks, J.A. (2014) Interactions between nitrogen, phosphorus, and molybdenum in forest soils and cyanobacterial lichen in the Oregon Coast Range, MS thesis. Oregon State University, p. 171.

McBride, M.B. (1994) Environmental chemistry of soils. Oxford University Press.

McManus, J., Berelson, W.M., Severmann, S., Poulson, R.L., Hammond, D.E., Klinkhammer, G.P. and Holm, C. (2006) Molybdenum and uranium geochemistry in continental margin sediments: Paleoproxy potential. Geochimica Et Cosmochimica Acta 70, 4643-4662.

Mikutta, R., Schaumann, G.E., Gildemeister, D., Bonneville, S., Kramer, M.G., Chorover, J., Chadwick, O.A. and Guggenberger, G. (2009) Biogeochemistry of mineral-organic associations across a long-term mineralogical soil gradient (0.3-4100 kyr), Hawaiian Islands. Geochimica Et Cosmochimica Acta 73, 2034-2060.

Miller, A.J., Schuur, E.A.G. and Chadwick, O.A. (2001) Redox control of phosphorus pools in Hawaiian montane forest soils. Geoderma 102, 219-237.

Moune, S., Sigmarsson, O., Schiano, P., Thordarson, T. and Keiding, J.K. (2012) Melt inclusion constraints on the magma source of Eyjafjallajokull 2010 flank eruption. Journal of Geophysical Research-Solid Earth 117.

Nagler, T.F., Anbar, A.D., Archer, C., Goldberg, T., Gordon, G.W., Greber, N.D., Siebert, C., Sohrin, Y. and Vance, D. (2014) Proposal for an International Molybdenum Isotope Measurement Standard and Data Representation. Geostandards and Geoanalytical Research 38, 149-151.

Neubert, N., Heri, A.R., Voegelin, A.R., Nagler, T.F., Schlunegger, F. and Villa, I.M. (2011) The molybdenum isotopic composition in river water: Constraints from small catchments. Earth and Planetary Science Letters 304, 180-190.

Neubert, N., Nagler, T.F. and Bottcher, M.E. (2008) Sulfidity controls molybdenum isotope fractionation into euxinic sediments: Evidence from the modern Black Sea. Geology 36, 775-778.

Opfergelt, S., Burton, K.W., Georg, R.B., West, A.J., Guicharnaud, R.A., Sigfusson, B., Siebert, C., Gislason, S.R. and Halliday, A.N. (2014) Magnesium retention on the soil exchange complex controlling Mg isotope variations in soils, soil solutions and vegetation in volcanic soils, Iceland. Geochimica Et Cosmochimica Acta 125, 110-130.

43

Orradottir, B., Archer, S.R., Arnalds, O., Wilding, L.P. and Thurow, T.L. (2008) Infiltration in Icelandic Andisols: The role of vegetation and soil frost. Arctic Antarctic and Alpine Research 40, 412-421.

Page, A.L., Miller, R.H. and Deeney, D.R. (1982) Chemical and Microbiological Properties, Methods of Soil Analysis: part 2, second ed. ed. American Society of Agronomy and Soil Science, Madison, Wisconsin.

Pearce, C.R., Burton, K.W., von Strandmann, P., James, R.H. and Gislason, S.R. (2010) Molybdenum isotope behaviour accompanying weathering and riverine transport in a basaltic terrain. Earth and Planetary Science Letters 295, 104-114.

Pearce, C.R., Cohen, A.S., Coe, A.L. and Burton, K.W. (2008) Molybdenum isotope evidence for global ocean anoxia coupled with perturbations to the carbon cycle during the early Jurassic. Geology 36, 231-234.

Pett-Ridge, J.C. (2007) Mineral aerosol inputs, nutrient sources, and weathering processes in tropical soils of Puerto Rico and the Hawaiian Islands, Department of Earth Sciences PhD thesis. Cornell University, Ithaca, p. 218.

Pett-Ridge, J.C., Derry, L.A. and Barrows, J.K. (2009a) Ca/Sr and Sr-87/Sr-86 ratios as tracers of Ca and Sr cycling in the Rio Icacos watershed, Luquillo Mountains, Puerto Rico. Chemical Geology 267, 32-45.

Pett-Ridge, J.C., Derry, L.A. and Kurtz, A.C. (2009b) Sr isotopes as a tracer of weathering processes and dust inputs in a tropical granitoid watershed, Luquillo Mountains, Puerto Rico. Geochimica et Cosmochimica Acta 73, 25-43.

Pett-Ridge, J.C., Monastra, V., Derry, L.A. and Chadwick, O.A. (2007) Sources and behavior of uranium in soils along a Hawaiian chronosequence. Chemical Geology 244, 691-707.

Pogge von Strandmann, P.A.E., Burton, K.W., James, R.H., van Calsteren, P., Gislason, S.R. and Sigfusson, B. (2008) The influence of weathering processes on riverine magnesium isotopes in a basaltic terrain. Earth and Planetary Science Letters 276, 187-197.

Pogge von Strandmann, P.A.E., Opfergelt, S., Lai, Y.J., Sigfusson, B., Gislason, S.R. and Burton, K.W. (2012) Lithium, magnesium and silicon isotope behaviour accompanying weathering in a basaltic soil and pore water profile in Iceland. Earth and Planetary Science Letters 339, 11-23.

Porder, S., Hilley, G.E. and Chadwick, O.A. (2007) Chemical weathering, mass loss, and dust inputs across a climate by time matrix in the Hawaiian Islands Earth and Planetary Science Letters 258, 414-427.

Poulson, R.L., Siebert, C., McManus, J. and Berelson, W.M. (2006) Authigenic molybdenum isotope signatures in marine sediments. Geology 34, 617-620.

Rasmussen, C., Brantley, S., Richter, D.d., Blum, A., Dixon, J. and White, A.F. (2011) Strong climate and tectonic control on plagioclase weathering in granitic terrain. Earth and Planetary Science Letters 301, 521-530.

Reed, S.C., Cleveland, C.C. and Townsend, A.R. (2013) Relationships among phosphorus, molybdenum and free-living nitrogen fixation in tropical rain forests: results from observational and experimental analyses. Biogeochemistry 114, 135-147.

Riebe, C.S., Kirchner, J.W. and Finkel, R.C. (2003) Long-term rates of chemical weathering and physical erosion from cosmogenic nuclides and geochemical mass balance. Geochimica et Cosmochimica Acta 67, 4411-4427.

Scheiderich, K., Helz, G.R. and Walker, R.J. (2010) Century-long record of Mo isotopic composition in sediments of a seasonally anoxic estuary (Chesapeake Bay). Earth and Planetary Science Letters 289, 189-197.

Scholz, F., McManus, J. and Sommer, S. (2013) The manganese and iron shuttle in a modern euxinic basin and implications for molybdenum cycling at euxinic ocean margins. Chemical Geology 355, 56-68.

Schuur, E.A.G., Chadwick, O.A. and Matson, P.A. (2001) Carbon cycling and soil carbon storage in mesic to wet Hawaiian montane forests. Ecology 82, 3182-3196.

Scribner, A.M., Kurtz, A.C. and Chadwick, O.A. (2006) Germanium sequestration by soil: Targeting the roles of secondary clays and Fe-oxyhydroxides. Earth and Planetary Science Letters 243, 760-770.

Siebert, C., Kramers, J.D., Meisel, T., Morel, P. and Nagler, T.F. (2005) PGE, Re-Os, and Mo isotope systematics in Archean and early Proterozoic sedimentary systems as proxies for redox conditions of the early Earth. Geochimica Et Cosmochimica Acta 69, 1787-1801.

Siebert, C., McManus, J., Bice, A., Poulson, R. and Berelson, W.M. (2006) Molybdenum isotope signatures in continental margin marine sediments. Earth and Planetary Science Letters 241, 723-733.

Siebert, C., Nagler, T.F. and Kramers, J.D. (2001) Determination of molybdenum isotope fractionation by double-spike multicollector inductively coupled plasma mass spectrometry. Geochemistry Geophysics Geosystems 2, art. no.-2000GC000124.

Siebert, C., Nagler, T.F., von Blanckenburg, F. and Kramers, J.D. (2003) Molybdenum isotope records as a potential new proxy for paleoceanography. Earth and Planetary Science Letters 211, 159-171.

Sigfusson, B., Gislason, S.R. and Paton, G.I. (2008) Pedogenesis and weathering rates of a Histic Andosol in Iceland: Field and experimental soil solution study. Geoderma 144, 572-592.

Skulan, J.L., Beard, B.L. and Johnson, C.M. (2002) Kinetic and equilibrium Fe isotope fractionation between aqueous Fe(III) and hematite. Geochimica Et Cosmochimica Acta 66, 2995-3015.

Soil Survey Staff (2014) Keys to Soil Taxonomy, 12th ed. USDA-Natural Resources Conservation Service, Washington, D.C.

Stonestrom, D.A., White, A.F. and Akstin, K.C. (1998) Determining rates of chemical weathering in soils - solute transport versus profile evolution. Journal of Hydrology 209, 331-345.

Thompson, A., Ruiz, J., Chadwick, O.A., Titus, M. and Chorover, J. (2007) Rayleigh fractionation of iron isotopes during pedogenesis along a climate sequence of Hawaiian basalt. Chemical Geology 238, 72-83.

Tsukuda, S., Sugiyama, M., Harita, Y. and Nishimura, K. (2005) Atmospheric bulk deposition of soluble phosphorus in Ashiu Experimental Forest, Central Japan: source apportionment and sample contamination problem. Atmospheric Environment 39, 823-836.

Voegelin, A.R., Nagler, T.F., Pettke, T., Neubert, N., Steinmann, M., Pourret, O. and Villa, I.M. (2012) The impact of igneous bedrock weathering on the Mo isotopic composition of stream waters: Natural samples and laboratory experiments. Geochimica Et Cosmochimica Acta 86, 150-165.

Voegelin, A.R., Pettke, T., Greber, N.D., von Niederhausern, B. and Nagler, T.F. (2014) Magma differentiation fractionates Mo isotope ratios: Evidence from the Kos Plateau Tuff (Aegean Arc). Lithos 190, 440-448.

Wasylenki, L.E., Anbar, A.D., Liermann, L.J., Mathur, R., Gordon, G.W. and Brantley, S.L. (2007) Isotope fractionation during microbial metal uptake measured by MC-ICP-MS. Journal of Analytical Atomic Spectrometry 22, 905-910.

Wasylenki, L.E., Rolfe, B.A., Weeks, C.L., Spiro, T.G. and Anbar, A.D. (2008) Experimental investigation of the effects of temperature and ionic strength on Mo isotope fractionation during adsorption to manganese oxides. Geochimica Et Cosmochimica Acta 72, 5997-6005.

White, A.F., Blum, A.E., Schulz, M.S., Vivit, D.V., Stonestrom, D.A., Larsen, M., Murphy, S.F. and Eberl, D. (1998) Chemical weathering in a tropical watershed, Luquillo Mountains, Puerto Rico: I. Long-term versus short-term weathering fluxes. Geochimica et Cosmochimica Acta 62, 209-226.

Wichard, T., Mishra, B., Myneni, S.C.B., Bellenger, J.P. and Kraepiel, A.M.L. (2009) Storage and bioavailability of molybdenum in soils increased by organic matter complexation. Nature Geoscience 2, 625-629.

Wiederhold, J.G., Kraemer, S.M., Teutsch, N., Borer, P.M., Halliday, A.N. and Kretzschmar, R. (2006) Iron isotope fractionation during proton-promoted, ligand-controlled, and reductive dissolution of goethite. Environmental Science & Technology 40, 3787-3793.

Wiederhold, J.G., Teutsch, N., Kraemer, S.M., Halliday, A.N. and Kretzschmar, R. (2007) Iron isotope fractionation during pedogenesis in redoximorphic soils. Soil Science Society of America Journal 71, 1840-1850.

Wille, M., Nagler, T.F., Lehmann, B., Schroder, S. and Kramers, J.D. (2008) Hydrogen sulphide release to surface waters at the Precambrian/Cambrian boundary. Nature 453, 767-769.

Wu, C.H., Lo, S.L. and Lin, C.F. (2000) Competitive adsorption of molybdate, chromate, sulfate, selenate, and selenite on gamma-Al2O3. Colloids and Surfaces a-Physicochemical and Engineering Aspects 166, 251-259.

Xu, N., Braida, W., Christodoulatos, C. and Chen, J.P. (2013) A Review of Molybdenum Adsorption in Soils/Bed Sediments: Speciation, Mechanism, and Model Applications. Soil & Sediment Contamination 22, 912-929.

Zerkle, A.L., Scheiderich, K., Maresca, J.A., Liermann, L.J. and Brantley, S.L. (2011) Molybdenum isotope fractionation by cyanobacterial assimilation during nitrate utilization and N-2 fixation. Geobiology 9, 94-106.

Ziegler, K., Chadwick, O.A., Brzezinski, M.A. and Kelly, E.F. (2005) Natural variations of delta Si-30 ratios during progressive basalt weathering, Hawaiian Islands. Geochimica Et Cosmochimica Acta 69, 4597-4610.

Figure 1.

Figure 2.

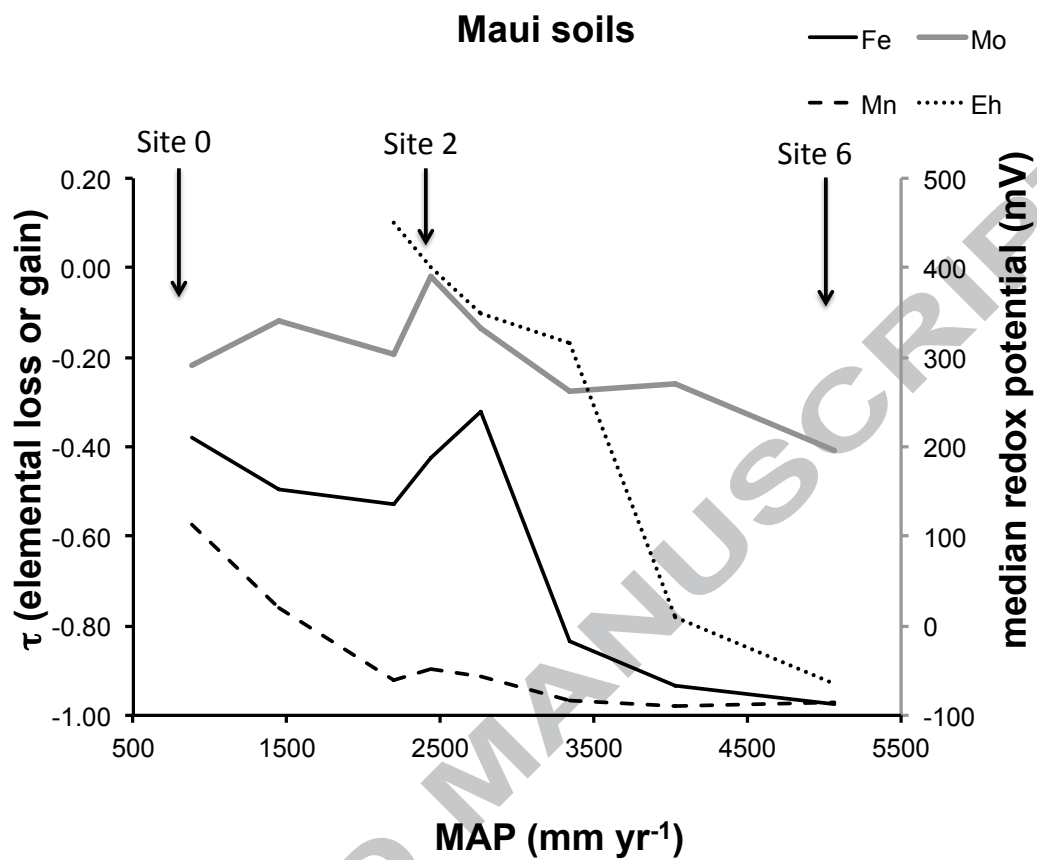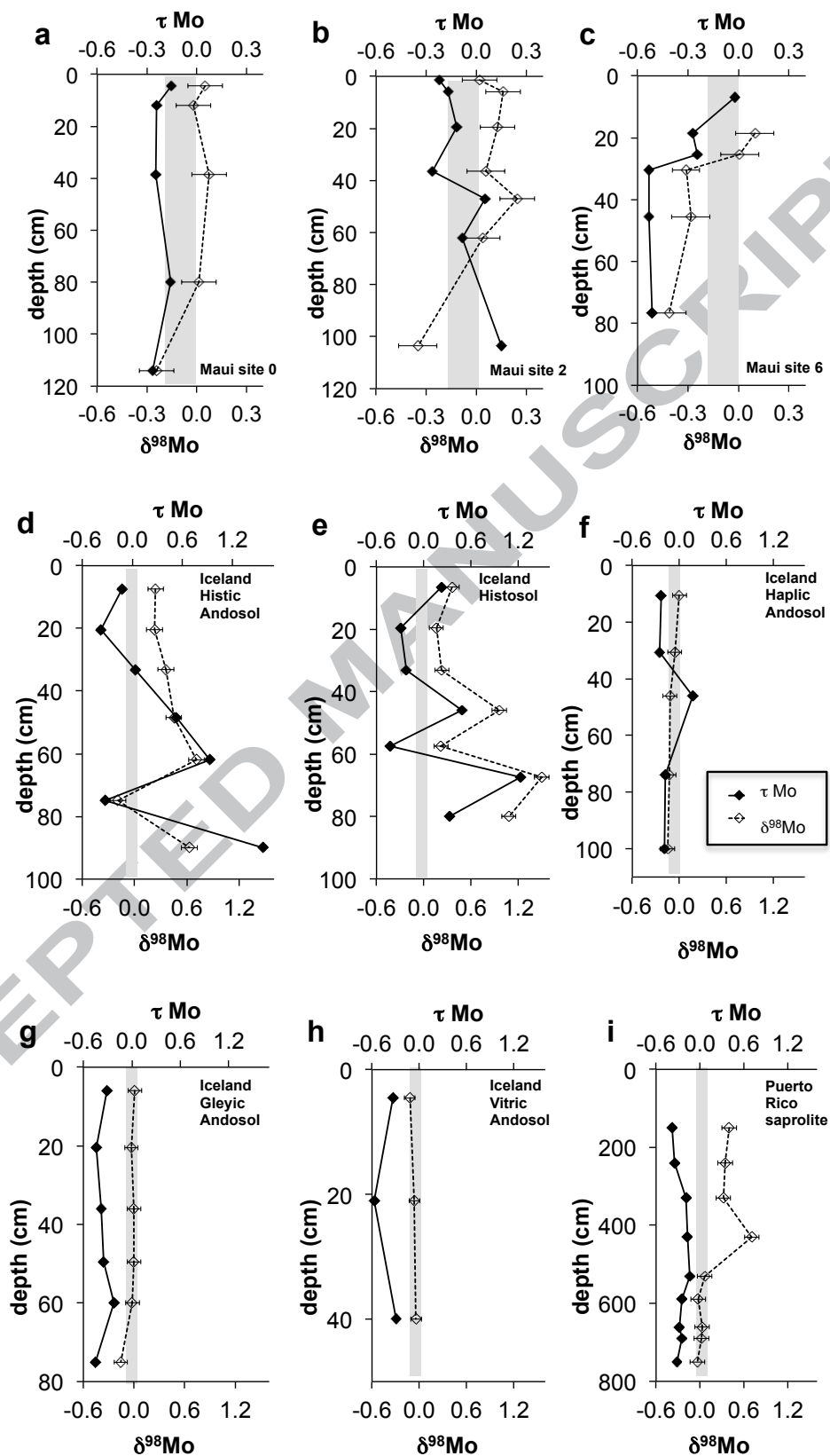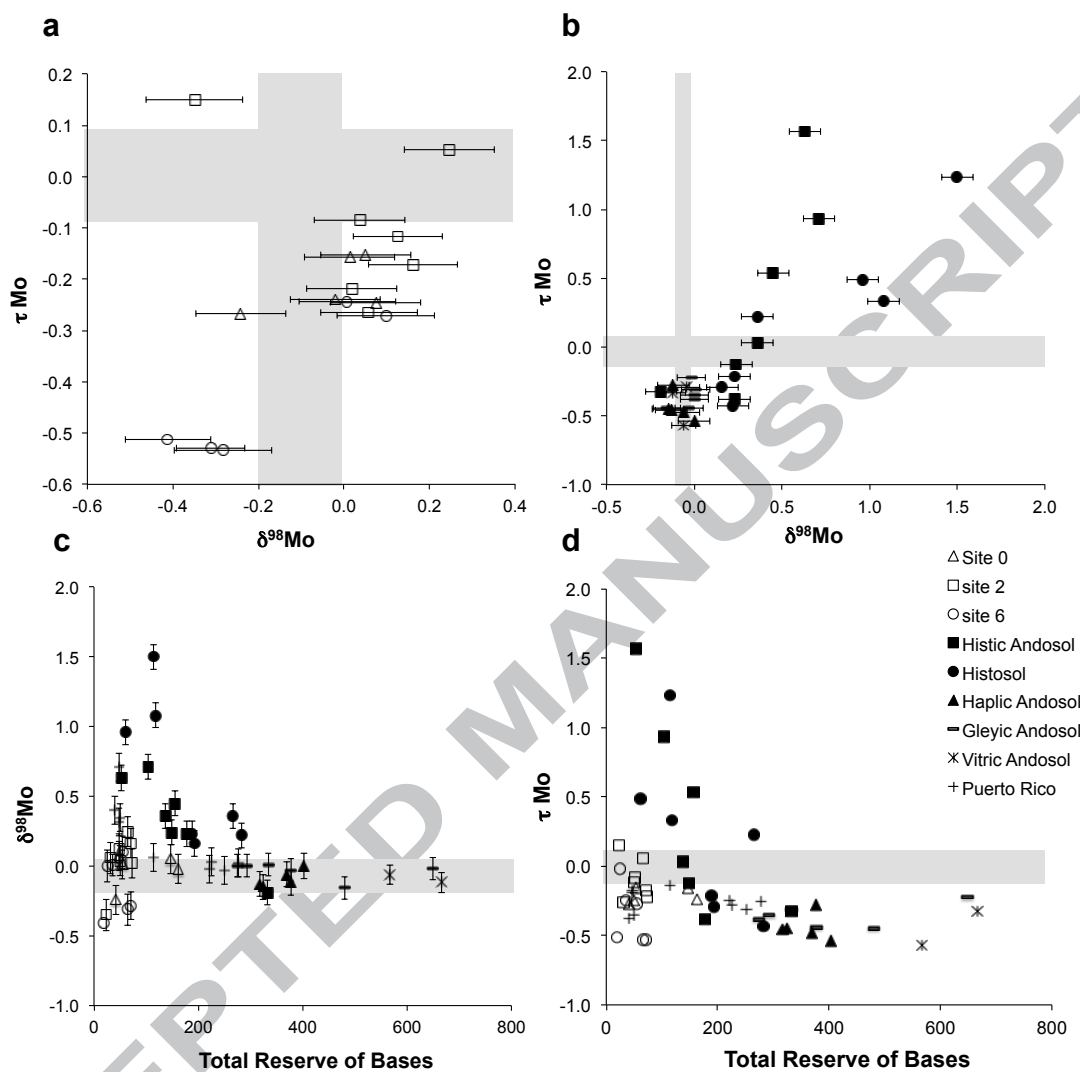**Figure 3.**

Figure 4.